

DYNAMIC INFLOW MODEL FOR HOVERING ROTORS IN NON-PARALLEL GROUND EFFECT

Jacopo Serafini, jacopo.serafini@uniroma3.it, Roma Tre University (Italy)
 Claudio Pasquali, claudio.pasquali@uniroma3.it, Roma Tre University (Italy)
 Giovanni Bernardini, giovanni.bernardini@uniroma3.it, Roma Tre University (Italy)
 Massimo Gennaretti, massimo.gennaretti@uniroma3.it, Roma Tre University (Italy)

Abstract

This paper presents a state-space dynamic inflow modeling method suitable for flight dynamics analysis of rotors in ground effect. Akin to the Pitt-Peters model, it relates inflow components to rotor loads as determined by a Vortex-Lattice-type numerical simulations, and may be applied to non-parallel rotor-ground configurations as well as to moving ground cases. Here, the model is identified for three flight hovering cases (far from the ground, near a parallel ground and near an inclined ground) and compared with a set of validation data, highlighting the capability of the proposed methodology to reproduce the main features of the inflow.

1. INTRODUCTION

Modern helicopter design and control development requires the availability of accurate dynamic inflow models to be included in solvers providing an effective computational support capable to simulate reliably the several complex aerodynamic environments in which rotors may operate. From decades, widely-used inflow models are those based on momentum theory, like the well-known Pitt-Peters⁶ and Peters-He⁵ ones. Originally developed for out-of-ground-effect rotor configurations, these models have been extended with some success to near-ground rotor operations through inclusion of a pressure perturbation from a specular rotor mirrored by the ground^{8,11}. However, the variety of possible in-ground-effect operation conditions (above inclined ground, moving ground, finite ground, non-flat ground, etc.) as well as the complexity of the corresponding aerodynamic field limit the validity of models based on analytical flow solutions.

This work proposes a dynamic inflow modelling approach for rotors in ground effects over both parallel and inclined surfaces, extracted from computational flow field simulations. Derived as a mod-

ification of the methodology introduced by some of the authors in the recent past³ to make it suitable for the specific issues related to the complexity of near-ground aerodynamics, a novel model identification process is first outlined and then applied. Conceived as a linear, time-invariant operator, the model is extracted through a multi-step procedure based on time-marching vortex-lattice method (VLM) simulations of the wake inflow. Forcing the wake structure system by suitable imposed vorticity distributions released at the trailing edges of the blades (related to the bound vortex circulation and hence to the sectional lift) and by trailing edge motion due to rotor rolling and pitching (known to be major causes of off-axis aerodynamic coupling¹), corresponding wake inflow and rotor loads are evaluated and the transfer functions between inflow coefficients and rotor loads (thrust, rolling and pitching moments) and rotor motion are identified.

Starting from the simulations given by a three-dimensional, free-wake computational tool applied to a mid-weight helicopter main rotor, the numerical investigation presents the results of the application of the inflow model identification methodology proposed for a rotor hovering above parallel and inclined ground.

Copyright Statement

The authors confirm that they, and/or their company or organization, hold copyright on all of the original material included in this paper. The authors also confirm that they have obtained permission, from the copyright holder of any third party material included in this paper, to publish it as part of their paper. The authors confirm that they give permission, or have obtained permission from the copyright holder of this paper, for the publication and distribution of this paper as part of the ERF proceedings or as individual offprints from the proceedings and for inclusion in a freely accessible web-based repository.

2. DYNAMIC INFLOW MODEL EXTRACTION

Similarly to the Pitt-Peters model⁶, the proposed modeling approach represents the perturbed wake inflow distribution over the rotor disc through the following expression in a non-rotating polar coordinate system, (r, ψ) ,

$$(1) \lambda(r, \psi, t) = \lambda_0(t) + r [\lambda_s(t) \sin \psi + \lambda_c(t) \cos \psi]$$

where r denotes distance from the disc centre, ψ is the azimuth angular distance from the aft position, whereas the coefficients λ_0 , λ_s and λ_c represent, respectively, instantaneous mean value, side-to-side and fore-to-aft gradients.

The perturbation inflow coefficients are assumed to be related to perturbation rotor thrust, roll and pitch moments (C_T, C_L, C_M), and to rotor pitch and roll angular velocities (p, q), through a state-space model, namely,

$$(2) \quad \dot{x} = Ax + Bu$$

where $u = \{C_T, C_L, C_M, p, q\}^T$ and x is such that

$$(3) \quad \lambda = \begin{Bmatrix} \lambda_0 \\ \lambda_s \\ \lambda_c \end{Bmatrix} = Cx$$

These coefficients are extracted through the following multi-step methodology: 1. starting from the trimmed steady-state solution, chirp-type perturbations of both vorticity released at the trailing edge of the blades and rotor motion are introduced; 2. the corresponding wake inflow on rotor blades is evaluated by free-wake, vortex-lattice simulations; 3. the corresponding aerodynamic loads are evaluated through a sectional aerodynamics model; 4. the transfer functions between rotor loads/motion and inflow coefficients are identified; 5. the rational approximation of transfer functions and the transformation back into time-domain yield the state-space dynamic model of the inflow coefficients.

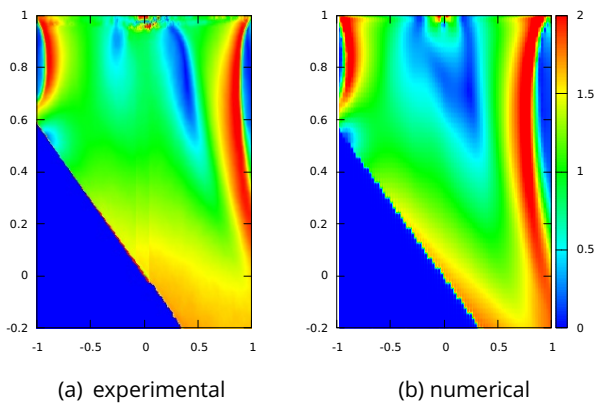
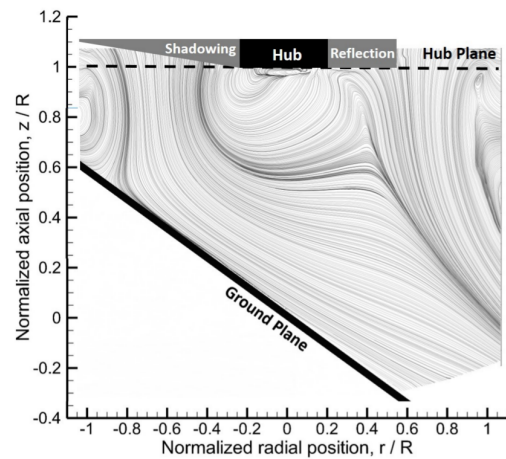


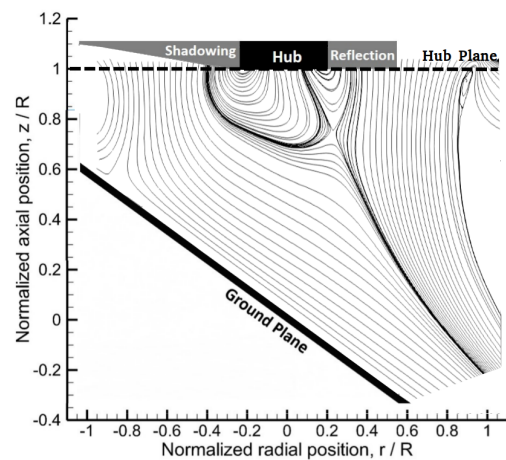
Figure 1: Flow-field velocity magnitude beneath the rotor for $\theta_g = 30^\circ$.

In the above process, ground effects on rotor aerodynamics are taken into account through the mirror image method, which is widely used in fluid-dynamics applications¹⁰. This approach has been

validated in the recent past against experimental data concerning a two-bladed rotor in hovering conditions over parallel and inclined ground⁴. As an example of the simulation capabilities of the aerodynamic solver applied here, Figs. 1 and 2 show comparisons between numerical and experimental data, respectively in terms of flow-field velocity magnitude and streamlines for a ground inclination angle equal to $\theta_g = 30^\circ$.



(a) experimental



(b) numerical

Figure 2: Streamlines beneath the rotor for $\theta_g = 30^\circ$.

Once the perturbed inflow (difference between actual inflow and reference steady-state one) is evaluated in response to perturbations of bound vorticity and rotor pitch and roll motion, λ_0 , λ_s and λ_c perturbation time histories are determined. To this purpose, the distribution of the bound vortex circulation, $\Delta\phi$, is modeled through the following first-order approximation

$$(4) \quad \Delta\phi(r, t) = r[\Delta\phi^0(t) + \Delta\phi^s(t) \sin \psi + \Delta\phi^c(t) \cos \psi].$$

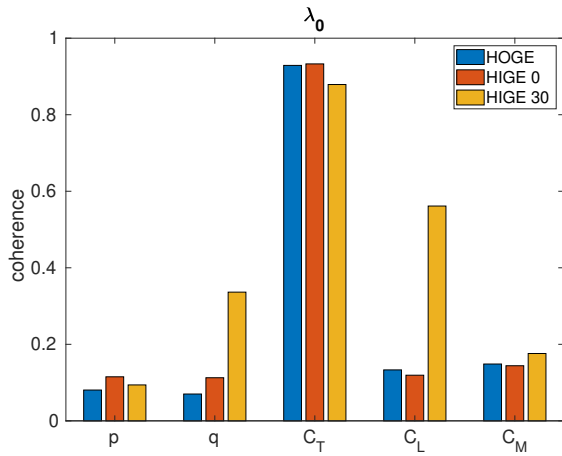
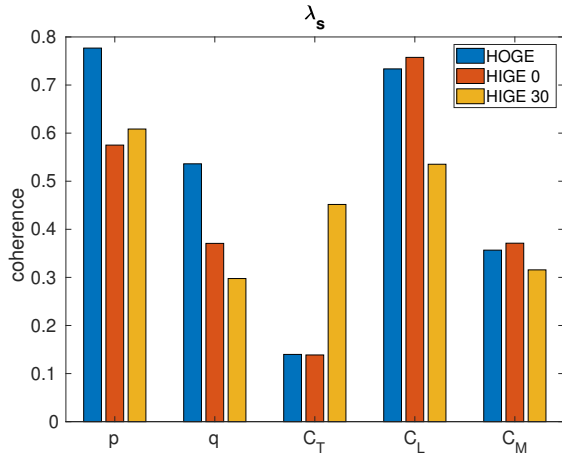
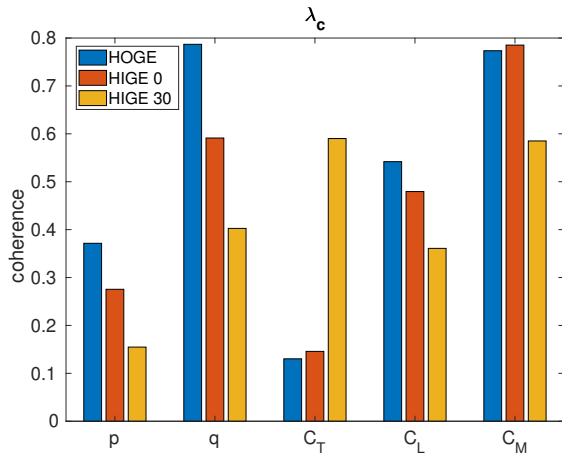
(a) λ_0 (b) λ_s (c) λ_c

Figure 3: Input-Output transfer function mean coherence for the three hovering conditions.

In the dynamic inflow model extraction process, in addition to the inflow, also rotor loads variations are determined as functions of $\Delta\phi^0$, $\Delta\phi^s$ and $\Delta\phi^c$ perturbations. Indeed, the integration the Glauert section load formula over the span of the blades yields the following one-to-one relation between $\Delta\phi$ coefficients and rotor load components, $\{C_T, C_L, C_M\}$,

$$\begin{aligned}
 C_T &= \sum_{j=1}^N \int_{e_h}^1 \frac{1}{\pi\Omega R^2} \bar{r} \Delta\phi(\bar{r}, t) d\bar{r} = \\
 &= \frac{N\Delta\phi^0(t) \bar{r}^3}{\pi\Omega R^2} \Big|_{e_h}^1 \\
 C_L &= \sum_{j=1}^N \int_{e_h}^1 \frac{1}{\pi\Omega R^2} \bar{r}^2 \sin \psi_j \Delta\phi(\bar{r}, t) d\bar{r} = \\
 &= \frac{N\Delta\phi^s(t) \bar{r}^4}{2\pi\Omega R} \Big|_{e_h}^1 \\
 C_M &= \sum_{j=1}^N \int_{e_h}^1 \frac{1}{\pi\Omega R^2} \bar{r}^2 \cos \psi_j \Delta\phi(\bar{r}, t) d\bar{r} = \\
 &= \frac{N\Delta\phi^c(t) \bar{r}^4}{2\pi\Omega R} \Big|_{e_h}^1
 \end{aligned}
 \tag{5}$$

where e_h is the nondimensional root-cut-off, N is the number of blades and \bar{r} denotes the nondimensional radial coordinate. Note that, when the rotor roll and pitch kinematics is perturbed, no load perturbations arise since bound vortex circulation is correspondingly left unperturbed. Then, combining loads and rotor kinematics perturbation with inflow coefficient perturbations corresponding to the same $\Delta\phi$ coefficients chirp-type perturbations, the $[3 \times 5]$ transfer functions relating \mathbf{u} to $\boldsymbol{\lambda}$ are identified.

The last step of the identification procedure is performed within the framework of the Matlab system identification toolbox. Here, in order to limit as much as possible the number of the variables involved in the identification process and taking into account the preliminary analysis of the coherence of each I/O relation shown in Fig. 3, for each element of the transfer functions matrix, the rational approximation has been obtained by including a number of poles and zeros that is in accordance with the extended Pitt-Peters theory¹. Thus, for hovering out-of-ground-effect and in-parallel-ground-effect conditions, the degrees of numerator and denominator polynomials of the transfer function rational approximations are as indicated in the following table

		C_T	C_L	C_M	ρ	q
(6)	λ_0	0/1	null	null	null	null
	λ_s	null	0/1	null	0/1	null
	λ_c	null	null	0/1	null	0/1

whereas for in-inclined-ground-effect conditions they become

		C_T	C_L	C_M	ρ	q
(7)	λ_0	1/2	null	0/2	null	0/2
	λ_s	null	0/1	null	0/1	null
	λ_c	0/2	null	1/2	null	1/2

The assumption in Eq. (7) derives from the consideration that, differently from the parallel-ground case, the inclined ground induces a fore-aft wake distortion similar to that caused by forward flight⁹ which, in turn, causes coupling between axial and non-axial pitching inflow/load parameters (see, for instance, the L_{13} and L_{31} coefficients of the Pitt-Peters model⁷), with the λ_s coefficient remaining still dependent of only rolling moment and angular velocity. As a proof of the asymmetric effect of inclined ground on the inflow, Fig. 4 shows the axial wake inflow on the rotor blades when they are orthogonal to the axis of rotation of the inclined ground. Starting from the parallel ground case $\theta_g = 0^\circ$, in which the radial distribution is almost symmetric, for increasing ground angle the numerical simulations show a reduction of the axial velocity in the uphill side and an opposite behavior in the downhill side (as expected from the flow blockage caused by ground when getting closer to the rotor, like in the uphill side).

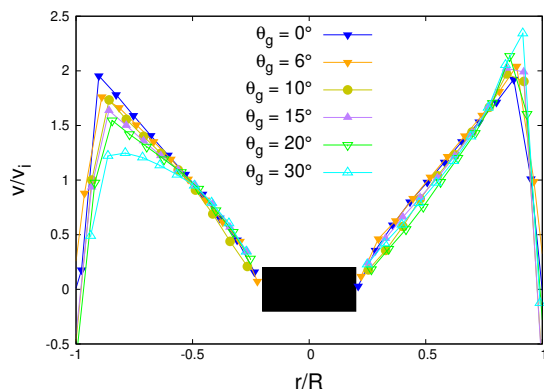


Figure 4: Axial wake inflow on rotor disk for $0^\circ \le \theta_g \le 30^\circ$.

The assumptions applied on the transfer functions matrix (shown in Figs. 6 and 7 for parallel and inclined ground, respectively) make the identification process more effective and robust. In particular, it is worth noting that the numerical simulations

have confirmed that the neglected transfer functions are actually negligible with respect to the remaining ones.

3. RESULTS

The test case considered is a mid-weight helicopter main rotor inspired to that of the Bo-105, whose main data are reported in 1, for hovering condition. Three configurations with different distances,

mass	2200	kg
MR type	hingeless	-
MR radius	4.91	m
MR chord	0.27	m
MR angular speed	44.4	rad/s
MR blade twist	-8	o/m
MR number of blades	4	-

Table 1: Main helicopter data

h_g , between rotor and ground and different ground inclination angles are analyzed: 1. out-of-ground-effect, in order to verify the capability of the proposed methodology to capture the main features of the problem; 2. in-ground-effect, with $h_g/R = 0.75$ and $\theta_g = 0^\circ$ (ground parallel to rotor disc), 3. in-ground-effect, with $h_g/R = 0.75$ and $\theta_g = 30^\circ$ (inclined ground) The frequency range of the analysis is limited to 1/rev (44.4 rad/s), which is well beyond the upper limit for flight dynamics applications. In the following, the main elements of the transfer functions matrix are presented and discussed.

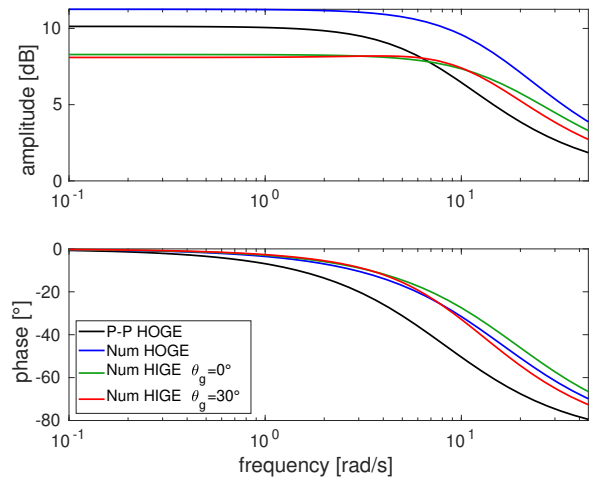


Figure 5: Magnitude and phase of C_T vs λ_0 transfer function: comparison between numerical data and Pitt-Peters analytic model.

First, for all the configurations analyzed, in Fig. 5 and Tab. 2 the numerical transfer function (HIGE

Case	poles [rad/s]	zeros [rad/s]
PP	-8.26	-
HOGE	-16.29	-
HIGE 0°	-19.26	-
HIGE 30°	-8.11, -11.87	-6.19

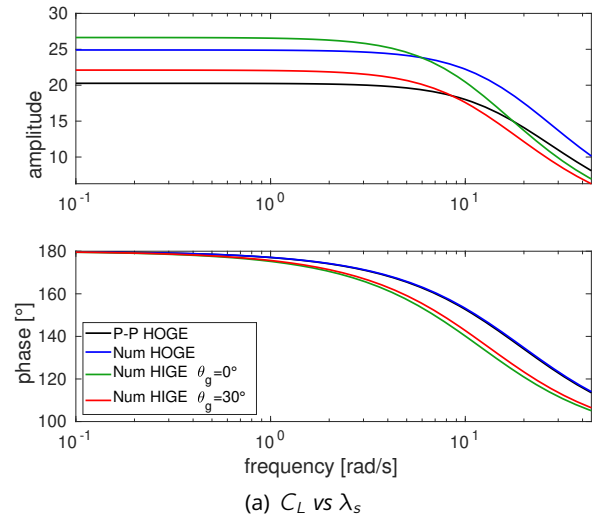
Table 2: Poles and zeros location of the C_T vs λ_0 transfer function: comparison between numerical data and Pitt-Peters analytic model.

and HIGE) between C_T and λ_0 and the location of its poles and zeros are shown and compared with those predicted by the Pitt-Peters model (PP) in out-of-ground-effect condition. With respect to the latter, the numerical HOGE transfer function surprisingly presents a significantly more damped pole, and then a significantly shorter time constant. On the contrary, the static gains are quite similar. Note that, for this particular transfer function, the Pitt-Peters model is known to be strongly dependent on the loads distribution along the blade span². Concerning the effects of the ground, it is evident that the ground increases the damping of the pole and slightly reduces the static gain. Furthermore, the transfer functions with inclined and parallel ground are very similar, even if the approximation process gives a quite different polynomial form, due to the different hypotheses on zeros and poles made in Fig. 6 with respect to Fig. 7. This result suggests the possibility of using one pole and no zeros to approximate this transfer function also in inclined-ground conditions.

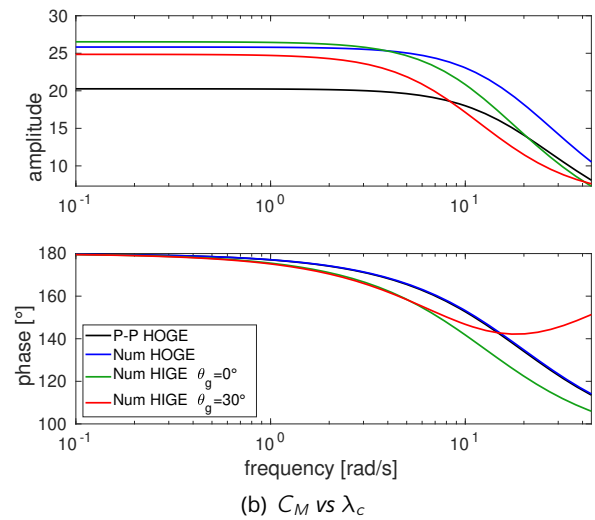
Then, Fig. 6(a) and Tab. 3 presents the results concerning the C_L vs λ_s transfer function. Also in this case, the following considerations may be drawn: 1. in out-of-ground effect conditions, the numerically identified transfer function has almost the same pole than the analytic Pitt-Peters' model. However, the transfer functions predicted by the two models present a difference in static gains of about 5 dB; 2. the presence of the ground significantly reduces damping, although the inclined-ground reduces it slightly less than the parallel-ground; 3. with respect to the HOGE case, the static gain of the transfer function increases in parallel-ground conditions (+2 dB) whereas it reduces (-3 dB) in inclined-ground ones.

Next, Fig. 6(b) and Tab. 4 presents the results regarding the C_M vs λ_c transfer function. As expected, the only remarkable differences with respect to the results presented in Fig. 6(a) and Tab. 3 occur in the inclined-ground case. Specifically, in this case, the identified transfer function has a pole significantly less damped than that of the C_L vs λ_s transfer function, and an additional highly damped one.

Finally, the synthesized inclined-ground per-



(a) C_L vs λ_s



(b) C_M vs λ_c

Figure 6: Magnitude and phase of transfer functions: comparison between numerical data and Pitt-Peters analytic model.

Case	poles	zeros [rad/s]
PP	-19.36	-
HOGE	-19.78	-
HIGE 0°	-11.98	-
HIGE 30°	-13.14	-

Table 3: Poles and zeros location of the C_L vs λ_s transfer function: comparison between numerical data and Pitt-Peters analytic model.

Case	poles	zeros [rad/s]
PP	-19.36	-
HOGE	-19.82	-
HIGE 0°	-12.69	-
HIGE 30°	-8.56, -10 ⁴	-34.94

Table 4: Poles and zeros location of the C_M vs λ_c transfer function: comparison between numerical data and Pitt-Peters analytic model.

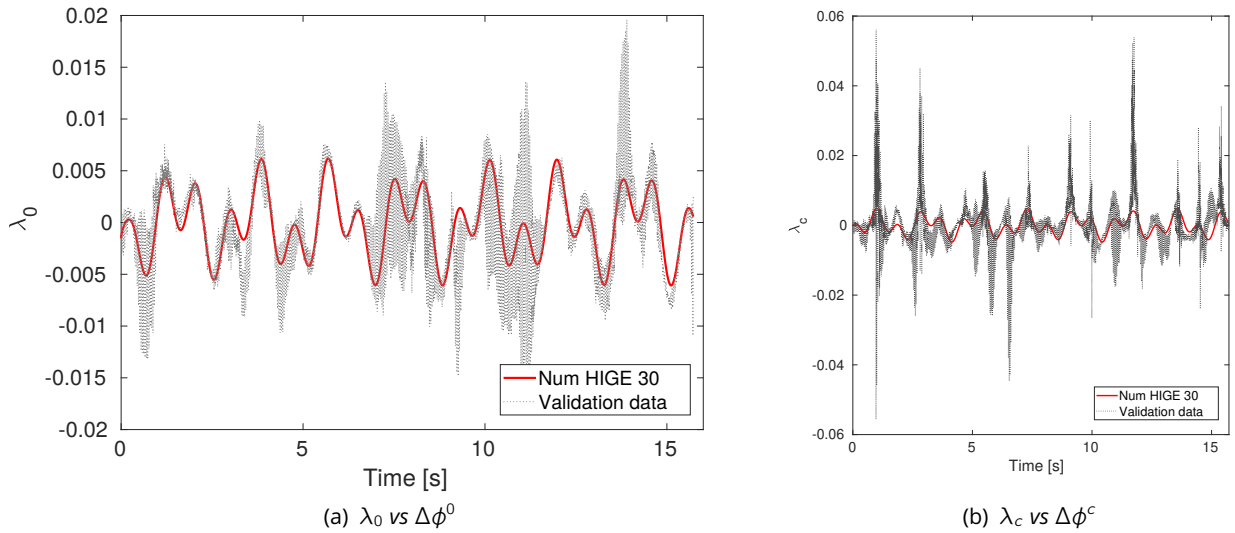


Figure 7: Time response: comparison between VLM simulations and state-space model predictions ($\theta_g = 30^\circ$).

turbed wake inflow model is verified against a validation data set numerically evaluated by imposing to the vortex-lattice aerodynamic solver an arbitrary perturbation to $\Delta\phi$ that is different from that used in the identification process. Specifically, Fig. 7(a) shows the responses of the vortex-lattice model and of the state-space formulation in terms of λ_0 to the following variation of the $\Delta\phi^0$ coefficient of the bound vortex circulation distribution

$$(8) \quad \Delta\phi^0(t) = \cos(5t)\sin(2t)$$

Note that, the rotor thrust coefficient perturbation corresponding to the circulation perturbation is used as the input of the wake inflow state-space model. Furthermore, Fig. 7(b) depicts the results in terms of the λ_c response to a perturbation of $\Delta\phi^c$ of the form of that in Eq. 8. Similarly to the results in Fig. 7(a), the corresponding perturbation of load (C_M in this analysis) is used as input to the state-space model.

In both cases, the identified model is capable of capturing with enough accuracy the low-frequency content of the inflow, which is the signal content mostly influencing the helicopter flight dynamics behavior. However, the validation signals present a relevant high-frequency contribution, as shown in Fig. 8, which depicts the spectrum of λ_0 . This figure highlights the tonal nature of the signal high-frequency content, which is clearly dominated by peaks around the multiple of the Blade Passing Frequency ($4/\Omega, 8/\Omega, \dots$), although two low-frequency peaks related to the perturbation frequencies in Eq. 8 arise (the introduction of a Linear Time Periodic inflow model would be necessary to

capture them).

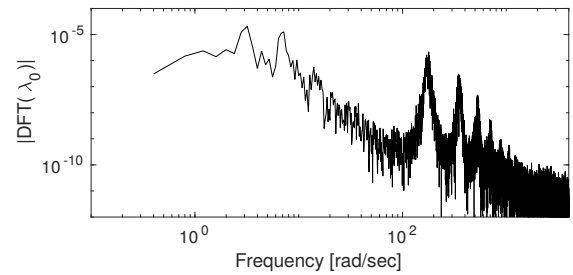


Figure 8: Spectrum of the λ_0 response to $\Delta\phi_0$ given by the VLM solver.

4. CONCLUSIONS

A methodology for the identification of a state-space dynamic wake inflow model for rotors in ground effect extracted from simulations provided by high-fidelity aerodynamic solvers has been developed and tested. It is based on inflow responses to chirp signals of blade bound vortex circulation distribution and of rotor rolling and pitching motion. The inflow is evaluated by a vortex-lattice solver which simulates the presence of the ground through a mirror image method. This method is sufficiently efficient to allow long simulations, which are required for a robust identification of the transfer functions relating inflow components to rotor loads and motion. The numerical investigation concerns the application of the proposed methodology for the wake inflow state-state model syn-

thesis of rotors both out-of-ground-effect and in-ground-effect conditions, above parallel and inclined grounds. The following conclusions may be drawn: 1. the mirror image is capable to model the main features of the flow around a rotor in ground effect, also when the ground is inclined with respect to the rotor disc; 2. the presence of the ground noticeably affects the wake inflow dynamic response; 3. the identification process requires long simulations, due to the presence of relevant numerical noise; 4. the validation tests show that the state-space model is capable of accurately reproduce the linear time invariant part of the low-frequency inflow content which is that significantly affecting flight dynamics. However, the wake inflow is also characterized by time-periodic phenomena, which cannot be reproduced by the proposed model, but would require the introduction of a time-periodic modeling approach.

ACKNOWLEDGEMENTS

This research was performed within the Roma Tre University participation in the University of Maryland/U.S.Naval Academy Vertical Lift Research Center of Excellence.

REFERENCES

- [1] U. T. Arnold, J. D. Keller, H. Curtiss, G. Reichert, et al. The effect of inflow models on the predicted response of helicopters. *Journal of the American Helicopter Society*, 43(1):25–36, 1998.
- [2] G. H. Gaonkar and D. A. Peters. Effectiveness of current dynamic-inflow models in hover and forward flight. *Journal of the American Helicopter Society*, 31(2):47–57, 1986.
- [3] M. Gennaretti, C. Pasquali, F. Cardito, J. Serafini, G. Bernardini, and R. Celi. Dynamic wake inflow modeling in ground effect for flight dynamics applications. In *AHS 73rd Annual Forum & Technology Display*, 2017.
- [4] C. Pasquali, J. Serafini, G. Bernardini, M. Gennaretti, J. Milluzzo, and S. Davids. Numerical-experimental correlation of rotor flowfield in ground effect. In *44th European Rotorcraft Forum (ERF 2018)*, 09 2018.
- [5] D. A. Peters and C. J. He. Correlation of measured induced velocities with a finite-state wake model. *Journal of the American Helicopter Society*, 36(3):59–70, 1991.
- [6] D. M. Pitt and D. A. Peters. Theoretical Predictions of Dynamic Inflow Derivatives. *Vertica*, 5:21–34, 1981.
- [7] D. M. Pitt and D. A. Peters. Rotor dynamic inflow derivatives and time constants from various inflow models. In *15th European Rotorcraft Forum: September 13-15, 1983, Stresa, Italy*, 1983.
- [8] H. Xin, J. Prasad, and D. Peters. Dynamic inflow modeling for simulation of a helicopter operating in ground effect. In *Modeling and Simulation Technologies Conference and Exhibit*, page 4114, 1999.
- [9] H. Xin, J. Prasad, D. Peters, N. Itoga, N. Iboshi, and T. Nagashima. Ground effect aerodynamics of lifting rotors hovering above inclined ground plane. In *17th Applied Aerodynamics Conference*, page 3223, 1999.
- [10] Y. Young and S. Kinnas. Analysis of supercavitating and surface-piercing propeller flows via bem. *Computational Mechanics*, 32(4-6):269–280, 2003.
- [11] H. Zhang, J. Prasad, and D. A. Peters. Finite state inflow models for lifting rotors in ground effect. In *Americas Helicopter Society - Annual forum; 52nd*, 1996.